Diyala Journal of Engineering Sciences

Journal homepage: https://djes.info/index.php/djes

ISSN: 1999-8716 (Print); 2616-6909 (Online)

Investigating 5G Wireless Networks Deployment with Diverse Frequency Bands for Basra City

Aymen M. Al-Kadhimi*

Department of Information and Communications Engineering, College of Information Engineering, AL-Nahrain University, Baghdad, Iraq

ARTICLE INFO

Article history:

Received September 5, 2024
Revised November 1, 2024
Accepted November 2, 2024
Available online December 1, 2024

Keywords:

5G
Cellular networks
Network planning
Network coverage
Network capacity

ABSTRACT

The emergence of Fifth Generation (5G) technology has marked a significant advancement in communication networks offering unique speed, capacity, and reliability. However, the successful deployment of 5G networks in urban environments requires careful consideration of various factors, including frequency band selection and infrastructure planning. Since Iraq has not yet witnessed the 5G network implementation, studying how the frequency bands vary and affect performance will provide insights into a smoother migration toward the next-generation cellular systems. This research aims to investigate the feasibility and potential benefits of deploying 5G wireless networks in Basra City utilizing a diverse range of frequency bands at 1.8, 2.1, and 3.6 GHz. A cellular network was designed and analysed to identify the most suitable frequency bands for 5G deployment in this Iraqi city as a case study which can be then generalized for other terrain-like regions. The site locations, antenna heights, transmission power, and antenna down-tilt degree were optimized through three design scenarios. Furthermore, four measurement themes were adopted to evaluate network performance as coverages, power levels, Carrier-to-Interference (C/I), and power density measurement themes. The results showed that despite the network with 3.6 GHz band slightly recorded lower levels of power density, the 1.8 GHz band proved its outperformance compared with the other two bands in terms of coverage, capacity, and C/I. Besides, the 1.8 GHz based design served almost 100 km^2 target area with excellent coverage. Consequently, the lower frequency 5G bands seemed to better accommodate users' demands in Basra City with the outlined constraints.

1. Introduction

For the last couple of decades, wireless cellular communications have exponentially expanded worldwide. Mobile communication has proceeded from being a luxurious technology exploited by some people to turn into a ubiquitous tool utilized by the vast majority of human beings these days [1]. Fifth-generation (5G) networks offer a substantial increase in capacity compared to their predecessors while accommodating a vast number of low-power devices and maintaining high reliability and low latency [2]. The expansion of 5G infrastructure necessitates the installation of new base stations to support the demands of future mobile services. A key challenge in deploying 5G networks is ensuring compliance with Electromagnetic Field (EMF) and spectrum regulations. Moreover, the transition from previous generations to 5G requires a corresponding adaptation of regulatory frameworks to address the unique

* Corresponding author.
E-mail address: aymen.mohammed@nahrainuniv.edu.iq
DOI: 10.24237/djes.2024.17404

technical specifications of the new technology [3].

Cellular networks, unlike other telecommunication techniques, are arranged into distinct generations, simplifying global standardization efforts. The first generation was primarily analog, with limited reach and data capabilities. 2G marked the advent of mass-market mobile telephony but had low data rates. 3G improved data rates and supported more data-intensive applications. 4G significantly increased data speeds that enabled a wider range of connected devices. The International Telecommunications Union (ITU) declares a bundle of technologies for improving wireless communications in terms of throughput speeds, coverage, and capacity to be aggregately called an Advanced Antenna System (AAS) [4], [5]. This collection of technologies is related to the 5G standard for mobile networking systems defined by the 3rd Generation Partnership Project (3GPP). AAS radios integrate antenna arrays with hardware and software to enable beamforming and spatial multiplexing. An important discrimination between AAS and traditional antennae is the number of supporting radio chains. A single radio is defined by its relevant equipment such as analog-to-digital or digital-to-analog converters, power amplifiers, and mixers. It is planned for the 5G to deploy 128-256 radio chains with no less than 64 transceivers integrated into one system [6]. Nevertheless, the application of 5G faces substantial challenges in network management, network planning, and network design. Those include determining the optimal base station placement, antenna configurations, as well as frequency assignment. The addressing of those tasks is important for gaining the entire potential of 5G technology.

Radio Network Planning (RNP) is a vital characteristic of cellular network design which ensures efficient allocation of resources among many active users. It involves the intentional placement of base stations to optimize network coverage with minimized costs. RNP depends on several factors such as environmental conditions, base station locations, pathloss propagation models, and frequency assignments [7]. Effective RNP results in fulfilled users and optimized infrastructure investment. The primary goal of RNP is to determine the optimal placement, arrangement, and configuration of base stations (BSs) to achieve maximum coverage of the network at the lowest cost. BSs should have the ability to serve mobile devices within their covered zones while keeping an acceptable call quality. RNP procedures must consider the propagation environments, site features, coverage and capacity requirements, and antenna configurations at all BSs. The 5G technology emerges new challenges and opportunities for RNP. The 5G systems present a modern core network and a new aerial interface known as the New Radio (NR) [8]. NR allows significantly higher throughputs and lower latency delays via utilizing innovative frequencies called the millimeter wave (mmW) [9]. These advancements demand advanced approaches to RNP to guarantee optimal performance and coverage in 5G networks.

5G networks adopt a heterogeneous architecture that includes BSs deployed near users in small cells that effectively reduce latency and assign active users with more resources to enhance network performance [7]. Furthermore, 5G systems implement active and sleep modes to optimize energy efficiency and minimize interference and power consumption. The 5G mmW frequencies are particularly suitable for wireless communications with short ranges to provide high throughputs and efficient operation in areas with dense populations. According to 3GPP, 5G operating bands are categorized into two Frequency Ranges: FR1 (450-6000 MHz) and FR2 (24.25-52.6 GHz) [10]. Many operators prioritize higher frequencies (i.e., FR2) to meet the growing capacity demands of densely populated areas. To ensure widespread coverage and support for all users, 5G systems require spectrum across three key frequency ranges: below 1 GHz, 1 to 6 GHz, and above 6 GHz.

The main objectives of this paper are outlined as follows:

1- Proposing a cellular 5G network design for Basra city. The design is optimized in terms of capacity and coverage to serve users within a target area.

2- Exploring how the variation in the 5G frequency bands affects network performance via deploying 1.8, 2.1, and 3.6 GHz bands (i.e., within FR1).
3- Analysing 5G network designs performance using different measures such as power levels, coverage ranges, interferences, and power densities.
4- Concluding the optimal frequency band that suits better the target region with declared constraints to attain a good performance.
5- Presenting an insight for network regulators or/ and operators to determine the most appropriate spectral allocations. That will unleash the full potential of 5G during migration from its predecessors.

2. Related works

The research conducted in [11] compared the signal strengths of 2G, 3G, and 4G cellular networks using smartphones with Android systems. Measurements were taken during a drive-test on a specific road at Ondokuz Mayis University. The results indicated that 2G signals were significantly stronger than 3G and 4G signals, and their strength varied based on location, frequency bands, line-of-sight alignment, and the power output of base stations. A separate study [12] evaluated the efficiency of Long-Term Evolution (LTE) base stations in rural and urban environments. This study specified that LTE BSs are more efficient in urban areas with smaller cell sizes under 750 meters. The performance of LTE telecommunications networks in Ghana and other Sub-Saharan African countries were investigated in [13] to explore the impact of desert terrain on antenna performance. The study resolved that a 2x2 Multi-Input Multi-Output (MIMO) antenna arrangement is optimal to cover such areas.

The importance of tailoring cellular network design to precise geographical characteristics of the deployment area was highlighted by the authors in [14]. They planned two lands: Baghdad as a flat region and Shaqlawa as a hilly region to highlight the impacts of terrain nature on network performance in terms of capacity and coverage metrics. The findings in [15] suggested that radio coverage optimization for LTE 800 cellular networks in urban locations often requires antenna parameters adjustments. These adjustments such as changing down tilt or height lead to signal propagation enhancement and overall network productivity. Furthermore, the simulations conducted in Indonesia and Cameroon [16, 17] offer valuable insights into the number of BSs needed to achieve acceptable coverage in LTE in various urban environments. Another investigation was carried out by the authors in [16] to reveal that 152 sites were required to attain 95% coverage of Semarang city whereas the realization of 244 sites was vital for Yaoundé city [17] to be covered with no less than -95 Decibel (dB) signals. These results highlighted the BSs' density should be wisely considered in zones with high population density or composite terrain to meet the defined coverage targets. The analysis for the spatial variability of signal strengths and data throughput within cellular networks was covered in [18]. The study's outcomes exposed a considerable attenuation of signal quality from the cell center to the border to raise challenges associated with steady performance sustainability throughout the whole target coverage district.

Wang et al. [19] introduced a smart strategy for planning cellular networks that not only saves costs but also ensures an even distribution of load. The authors aimed to improve the Quality of Service (QoS) with keeping resource utilization optimized. That was done by a reasonable adoption of low-power cells in target zones. A comprehensive LTE network design for Banepa City was developed in [20] to fulfill the increasing demand for high speeds of data and voice services. The study proposed seven 3-sector sites operating at the 1800 MHz frequency with accurate planning for capacity, coverage, and network parameters. Abdulhamid et al. [21] obtained a novel algorithm for automating network planning and optimization. It was designed to mitigate intra-system interference and adhere to key performance indicators. This algorithm regulated the mission of radio frequency engineers, reduced operational expenses, and facilitated cellular

network deployment. Moreover, the algorithm allows to implement networks with maximum quality, quantity, and coverage via planning process automation.

Since the mmWave frequencies suffer from higher propagation losses that limit the cell's site radius [22], a larger number of smaller cell sites are required. However, that increase in cellular sites results in higher radiation levels of EMF. Ahmed et al. [23] analysed the power density of a 5G network by proposing a deployment technique for a target area in Austin, Texas. They showed that there is a significant growth in exposure levels when upgrading LTE towers to 5G BSs. Another study [24] presented a 5G-NR network planning at mmWave. The target area was 5 km^2 of Pulogadung Indonesian state at 28 GHz. They used Mentum Planet to simulate 60 sites to ensure a reasonable level of service for the downlink. Furthermore, Sigit Kusmariyanto et al. [25] planned a 5G-NR cellular network based on 28 GHz band and 100 MHz bandwidth for Malang City. They demonstrated design performance in terms of capacity and coverage along with the required number of the Next-Generation Node Base stations (gNodeB) using the Atoll planning tool. This software is then equipped with an Artificial Intelligence (AI) module by the authors in [26]. The AI approach was developed based on the Long Short-Term Memory (LSTM) algorithm to build a forecasting model for analysing real-time traffic. This enhancement on the Atoll added smartness to the planning and optimization of mobile networks.

The previous studies have not compared and analysed the diverse frequency bands for 5G networks. This paper presents an intensive analysis of cellular networks designed and analysed to identify the most suitable frequency bands for 5G deployment in Basra Iraqi city. This case study can be then generalized for other terrain-like regions to help network regulators/ operators to gain insights on determining the most appropriate spectral allocations.

3. Empirical models for pathloss

Pathloss models are considered a fundamental component of radio propagation analysis. Empirical models for pathloss are mathematical formulations that estimate the attenuation of radio signals while propagation via space. This estimation considers factors such as distance, frequency, and environmental conditions. The models play a crucial role in the design and optimization of wireless communication systems as they provide valuable insights into signal propagation characteristics. Some of the well-known pathloss models are described in the next subsections [27].

3.1 Free space path losses

The free space pathloss model describes the ideal attenuation of a radio signal in the absence of any obstacles. This model serves as a baseline to understand the inherent signal degradation that occurs due to the natural spreading of electromagnetic waves. The pathloss is determined as:

$$PL_{Free}(dB) = 20\log_{10}(d) + 20\log_{10}(f) + 32.4 \quad (1)$$

where d is the transmitter-to-receiver distance in kilometres and f is the frequency in megahertz. The 32.4 is a constant obtained from converting the term $4\pi c$ from linear scale to dB where c is the speed of light.

3.2 Cost Hata model

This propagation model is particularly customized to operate with frequencies between 1.5 GHz and 2 GHz to be commonly employed in urban and suburban environments. It involves empirical data to account for the complex propagation conditions encountered in these areas, providing more accurate predictions than the free space approach. These kinds of path losses are obtained as:

$$PL_{\text{Cost}}(dB) = 46.3 + 33.9\,log_{10}(f) - 13.82\,log_{10}(h_b) - ah_r + (44.9 - 6.55\log 10(h_b))\,log_{10}(d) \quad (2)$$

where d is the transmitter-to-receiver distance in kilometres, f is the frequency in megahertz, a represents a correction factor, h_b and h_r are the antenna heights of the base station and receiver, respectively. The h_b usually takes the values 30-200 meters whereas h_r is equal to 1-10 meters.

3.3 Okumura-Hata Model

The Okumura-Hata model is widely recognized and endorsed by the ITU. It is a versatile model applicable for frequencies up to 3.5 GHz. A comprehensive method to pathloss prediction is offered by this model to contribute various environmental factors and provide reliable estimates over broad ranges of operating conditions. The pathloss of one cell with this model is calculated as:

$$PL_{\text{Okum}}(dB) = 69.55 + 26.16\log_{10}(f) - 13.82\,log_{10}(h_b) - ah_r + \left(44.9 - 6.55log_{10}\,(h_b)\right)log_{10}\,(d) \quad (3)$$

where f, d, a, h_r, and h_b parameters are previously defined above. The constants shown in Eq. (2) and Eq. (3) are parts of the empirical modeling used for helping to adjust the overall path loss prediction for real-world observations.

3.4 Erceg model

This pathloss propagation model is precisely intended for urban microcellular environments which considers parameters such as street orientation, building density, and the impacts of shadowing. It is typically limited to frequencies between 800 and 3700 MHz, base station antenna heights of 10 to 80 meters, mobile heights of approximately 2 meters, and cell ranges of 0.1 to 8 kilometres. The Erceg model was proposed by Victor Erceg [28] and defined by the IEEE 802.16.3c standard for WiMAX planning. It is designed for suburban and urban areas and categorizes Non-line-of-Sight (NLoS) scenarios into three types: Type A, Type B, and Type C. The terrain Type A emulates the highest pathloss compared with the other two types because it describes a hilly region with a heavily tree-dense nature. On the other hand, Type C is associated with the lowest pathloss for a flat area with sparse tree distribution. The remaining Type B produces a moderate loss in between the other two terrain types.

In this paper, the Erceg propagation model is applied for pathloss approximation among the 5G networking sites of the presented design via utilizing WiMAP radio planning software. The propagation model is adopted to perform measurements since it allows differentiation among diverse kinds of terrestrial structures. Particularly, the Type-C is employed for 5G network planning for Basra City whose terrain is generally flat with a sparse tree existence. Basra City, with its strategic location and growing population, presents a unique opportunity and challenges for 5G network deployment. The city's geographic terrain is flat with some marshlands and coastal areas. Additionally, its port activity makes it crucial to prioritize coverage there to support maritime communications and logistics. However, the extreme weather conditions of Basra such as high temperatures, humidity, and dust may impact network performance quality.

4. Network design method

4.1 Design flowchart

The flowchart shown in Figure 1 outlines the process steps of the cellular network design and optimization. It begins with a definition and analysis of the network's requirements. This stage serves as the foundation for the subsequent steps. Then, the WiMAP tool is adopted to design the initial cellular network configuration. The optimization phase crucially comes next to enhance network performance via various parameter adjustments. These parameters may include the BSs' locations, channel allocation strategies, transmit power levels, and antenna tilt and height settings. The goal of optimization is to achieve the best possible network coverage, capacity, and QoS while taking the cost and interference into consideration.

Once the network optimization is completed, the design undergoes the testing and calculation phase for performance assessment against the requirements defined earlier. If the requirements are met, the process accomplishes successfully. However, if the requirements are not fulfilled, the flowchart loops back to the optimization step to allow for further adjustments and refinements until the desired performance is achieved. This iterative approach confirms that the final cellular network is well designed to meet the specific needs and challenges of the target area which in turn results in a more robust and efficient communication infrastructure.

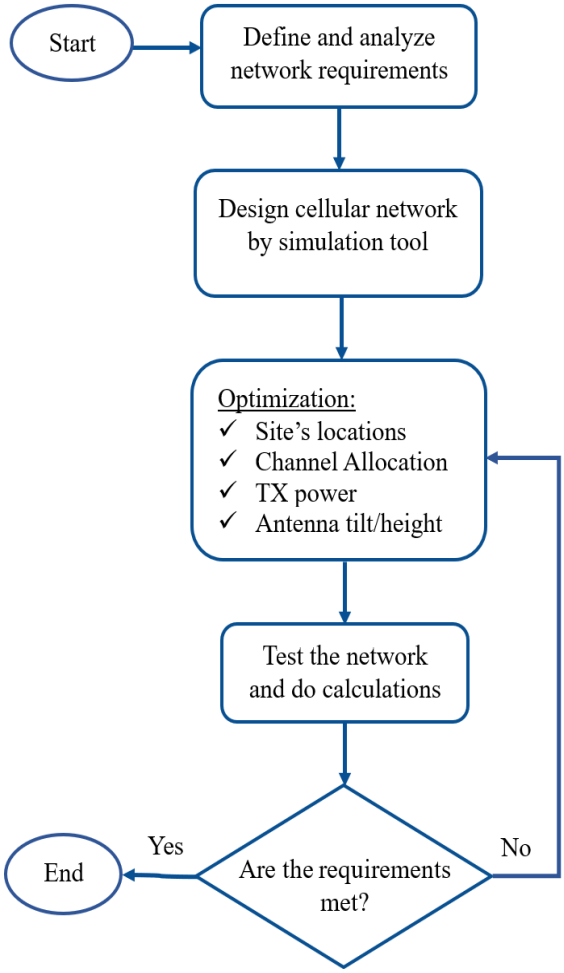

Figure 1. Network design flowchart

4.2 Design definition and assumptions

The design objective is to offer 5G cellular services with optimized capacity and coverage for Basra City and analyze the effects of deploying diverse frequency bands. The FR1 bands, specifically 3.6 GHz, 2.1 GHz, and 1.8 GHz, are applied in the proposed design. The target is to serve a geographical area of approximately 100 km^2 (i.e., a radius of 5653 meter) that is depicted in Figure 2. This specific target area is considered because there are a maximum number of 12 base stations allowed by the simulation tool. Since the Basra city is considered a low-dense tree and flat region, the Erceg Type C is assumed as the propagation model when doing the calculations.

The network mainly includes four types of equipment: sites, antennae, clients, and points. A site represents a cellular base station each equipped with several antennae to cover 360° direction in most scenarios. That requires 120° individual coverage by three antennae arrangements. Furthermore, for the purpose of doing the power measurements and Carrier to Interference ratios (C/I), several clients and points are reasonably placed across the network design. In addition, the coverage probability, utilization, thermal noise density, and noise figure are assumed to be equal to 50%, 50%, -174 dBm/Hz, and 3 dB, respectively. These numbers are chosen in this study as a normal and fair general assumption. For the sites' height and transmitting power, they are defined accordingly depending on the adopted 5G frequency band as shown in the next section. Generally, higher-frequency waveforms have shorter wavelengths and are more susceptible to attenuation which in turn limit their range. To compensate for this, a higher transmit power is usually applied. In consequence, the 3.6 GHz based design is assigned with the highest transmit power (in dBm) among other bands. On the contrary, the least dBm of power is set for the network design with the 1.8 GHz band.

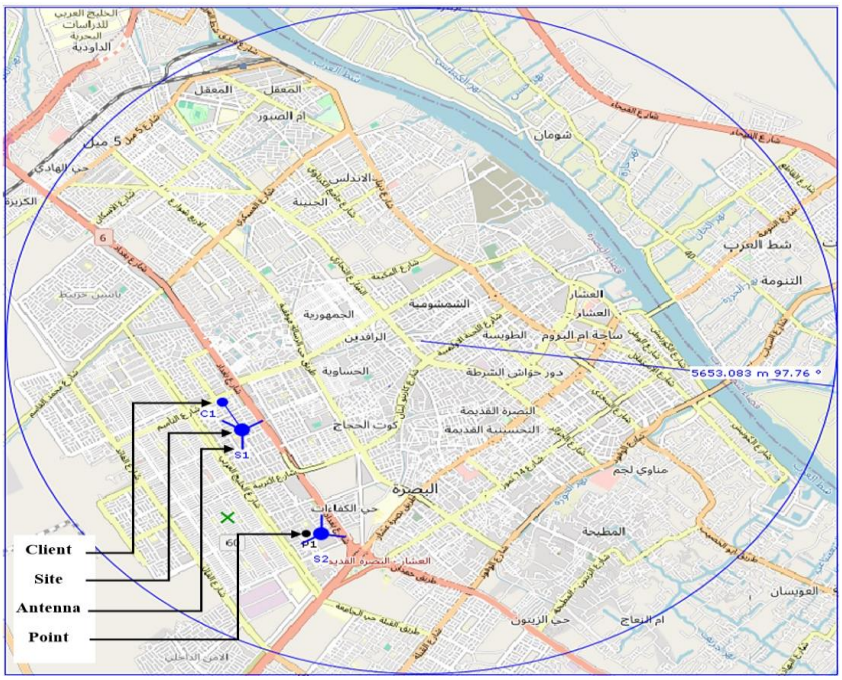

Figure 2. General network layout

5. Results and discussion

Three 5G frequency bands are investigated in the proposed network design. Each deployment is optimized and evaluated using several measurements to assess the network coverage and service level.

5.1 5G Network Deployment with 3.6 GHz Band

The first design scenario adopts 3.6 GHz with the network optimized placement shown in Figure 3. There are 12 sites (S1 through S12) each equipped with 3 antennae except S7 which comes with 2 antennae since it is located at the boundary of the coverage target. Each antenna is mounted at 16.4 m above ground and transmits with a power of 53 dBm. The antennae down tilt is set to zero and their azimuth (i.e., direction degree) changes per site to get the reasonable optimized coverage.

To start testing the proposed network design, several calculations are examined. Initially, coverage measurements are observed at 2 m above the ground as shown in Figure 4. The blue region indicates areas with excellent coverage whereas green shading still refers to good services. Even though the users in the yellow areas have limited connection, they cannot experience any coverage if they move to the unshaded spots. Moreover, it is noticeable that the closest users to sites get served the most. There is still an acceptable handover among sites to handle mobility. Overall, the majority of the target area is reasonably covered at this calculation height. Furthermore, the height above ground is increased to 20 m to assess its impact on coverage calculation as shown in Figure 5. As can be seen, the vast majority of the network becomes in blue which translates to excellent coverage. That is because when raising the calculation height, a Fresnel zone is offered with Line of Sight (LOS) due to avoiding the obstacles compared with the 2 m case which may block some signals while transmission. Figure 6 outlines that fact as it shows that elevation between the S5-P2 path at 20 m above ground has a LOS with no obstacles compared with the same path at 2 m as shown in Figure 7. However, the most practical scenario is when doing calculations at 2 m since it emulates the normal user height.

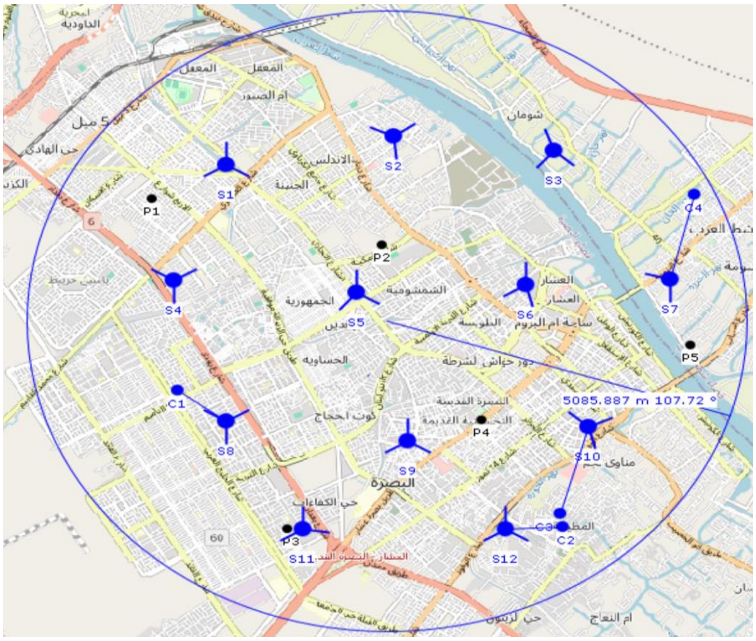

Figure 3. Network design at 3.6 GHz

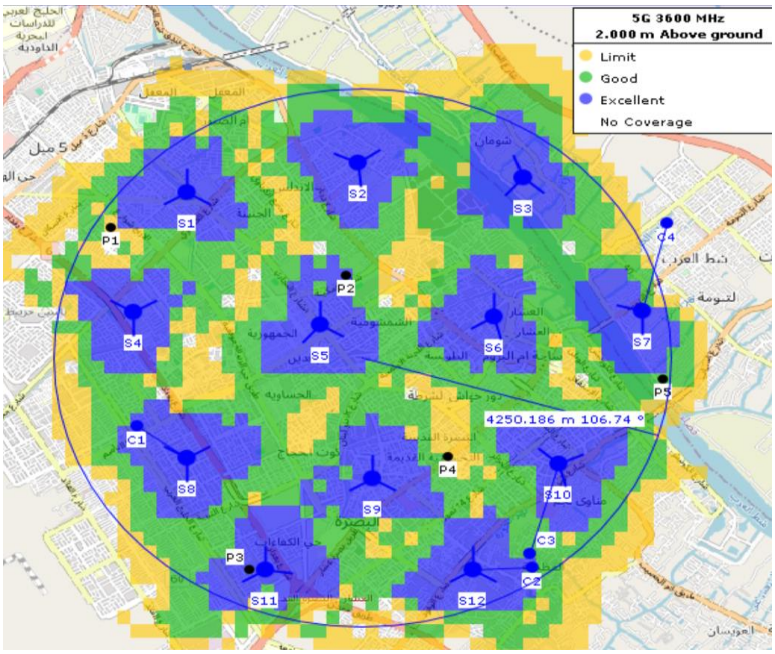

Figure 4. 3.6 GHz Coverage calculation at 2m above ground

The following calculation involves power levels evaluation. As can be seen in Figure 8, the power intensity level varies across the network such that the yellow shading is equivalent to -70 dBm while the reddish refers to low power levels at <-100 dBm. In addition, the greenish spots located very close to the sites record the best power at >-40 dBm. To have more adequate power readings, five points (P1 through P5) are spread throughout the network to reveal measurement levels listed in Table 1. The highest power level, among those five placed points, is recorded by P3 at -79.3 dBm whereas P4 experiences the lowest at -127.3 dBm. That is determined based on the points' placement proximity from their corresponding serving sites. Then, the calculation is investigated at 20 m above ground in Figure 9 to unleash power levels enhancement with wider green and yellow spots. That increase in power is due to calculation elevation rise from 2 m to 20 m above ground which means less blockage by obstacles.

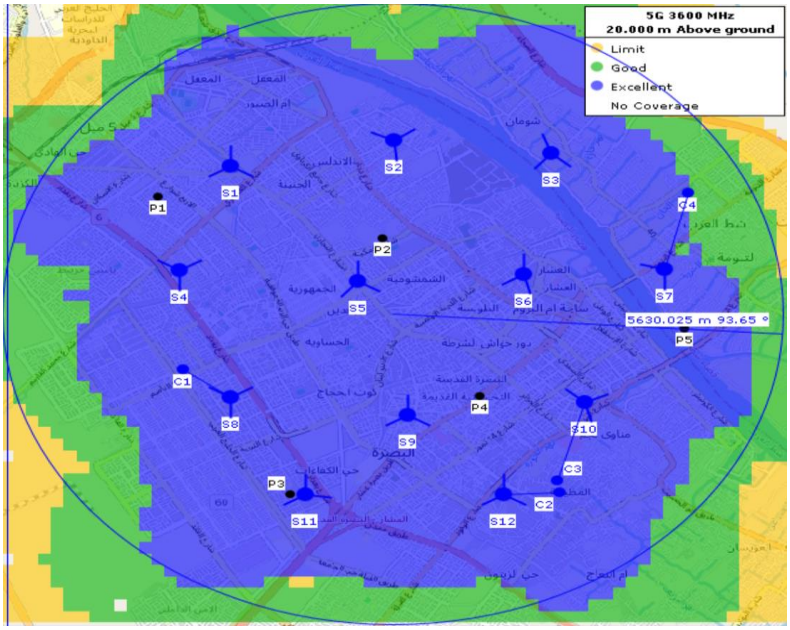

Figure 5. 3.6 GHz Coverage calculation at 20m above ground

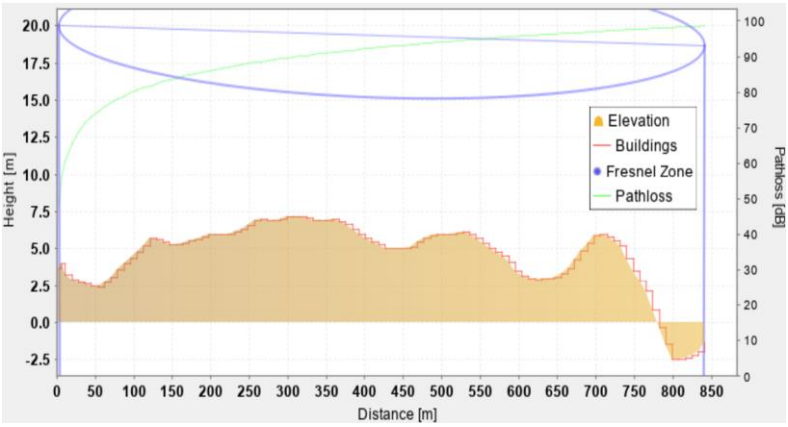

Figure 6. S5-P2 path elevation at 20m above ground

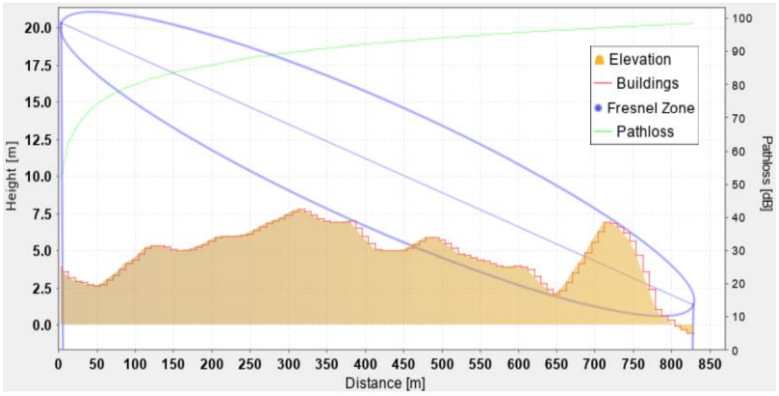

Figure 7. S5-P2 path elevation at 2m above ground

Table 1: 3.6 GHz point power levels at 2m above ground

Point	Power (dBm)
P1	-124.4
P2	-119.1
P3	-79.3
P4	-127.3
P5	-114.6

The Carrier-to-Interference ratio (C/I) is a vital indicator used in network planning, particularly for wireless cellular communication systems. It is essential for assessing the quality of service (QoS) and optimizing network performance. C/I is the ratio of the power of the desired signal (carrier) to the power of the interfering signals. A high C/I value specifies that the desired signal is stronger relative to the interfering signals, resulting in an improved signal quality with fewer dropped calls or data interruptions. The C/I calculation of the proposed 3.6 GHz based design is shown in Figure 10. The majority of spots near the sites are shaded in green with C/I greater than 20 dB which reveals a low level of interference. In other words, users located in greenish areas are offered better QoS as they do not suffer from carrier interference unlike those who stand in yellowish regions that involve higher interference. Even though the presence of reddish areas indicates potential interference issues at C/I of less than -10 dB, the network design does not show any of those areas but some orange spots that are still minimized.

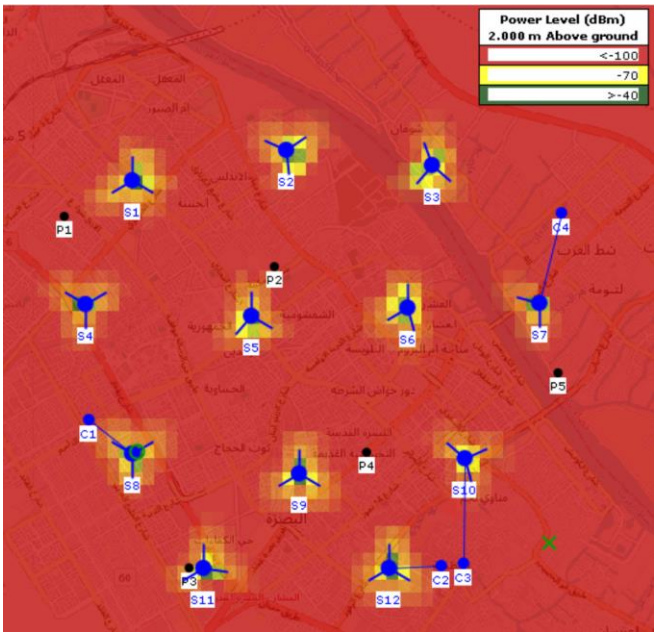

Figure 8. 3.6 GHz power calculation at 2m above ground

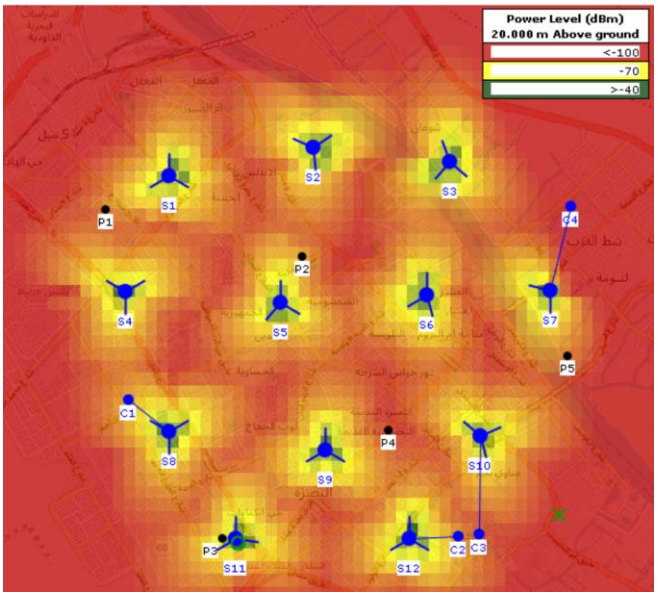

Figure 9. 3.6 GHz power calculation at 20m above ground

While it's technically feasible to estimate power levels and coverage directly from a map, more accurate and precise results can be obtained by conducting client calculations at specific real-world locations. Each client is assigned to a serving site within the network. To measure coverage, received power, and interference levels, several clients were intentionally placed throughout the network, as illustrated in Table 2. Among the clients evaluated, the client (C1) exhibited the strongest received power at -81.5 dB while maintaining a minimal interference level at -12.5 dB as C/I. Conversely, client (C4) received the weakest power level of -101.1 dB, accompanied by a C/I of -19.2 dB since it is positioned far at the perimeter of the target coverage area. Furthermore, the C3 experiences the highest C/I among other clients at -25.3 dB which indicates heavy interference by adjacent client C2 and site S12. More clients can be added throughout the network but four clients seem to be sufficient to get a reasonable indication. In essence, clients located closer to sites experience better C/I and power levels.

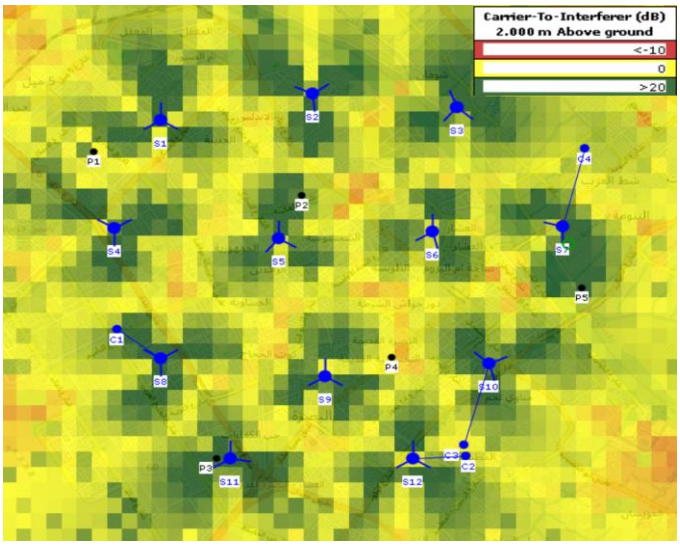

Figure 10. 3.6 GHz interference levels determination

Table 2: 3.6 GHz clients' calculations

Client	Received Power (dB)	C/I (dB)
C1	-81.5	-12.5
C2	-85.3	-17.7
C3	-89.5	-25.3
C4	-101.1	-19.2

The measurement of field strength is crucial for assessing power density levels in areas surrounding antennas. This information is essential to ensure compliance with safety regulations and prevent potential health risks associated with excessive exposure to electromagnetic radiation. High power density can pose a threat to human health, emphasizing the importance of regularly monitoring field strength levels and ensuring that critical values are not exceeded. Figure 11 indicates the power density levels in microwatt per square meter ($\mu W/m^2$) calculated across the designed network. The measurement was done 2 m above ground to assess the Root Mean Square (RMS) values. It can be seen that the power density in most of the regions across the network is kept minimum at less than 1 $\mu W/m^2$. The power density near some sites' antennae records 3-800 $\mu W/m^2$. On the other hand, to investigate the extreme situations with a maximum load in the network, Figure 12 witnesses an increase in power density levels around and close to sites compared with the base load. That is due to considering heavy traffic by users with maximum load on network infrastructure which is an extreme case scenario not usually involved in reality.

5.2 5G Network Deployment with 2.1 GHz Band

In this section, a second network scenario is designed at a 2.1 GHz frequency band. To maintain fairness while comparing different frequency bands, the sites' placements are kept as they were in the first design except for two changes. The antennae height was set to 27.8 m above ground to transmit signals with a power of 46 dBm. That leads to 7 dBm less power consumption compared to the 3.6 GHz network. That is because higher frequency bands experience more signal attenuation due to factors like atmospheric absorption, building penetration, and foliage [29] which require the sites to raise transmission powers.

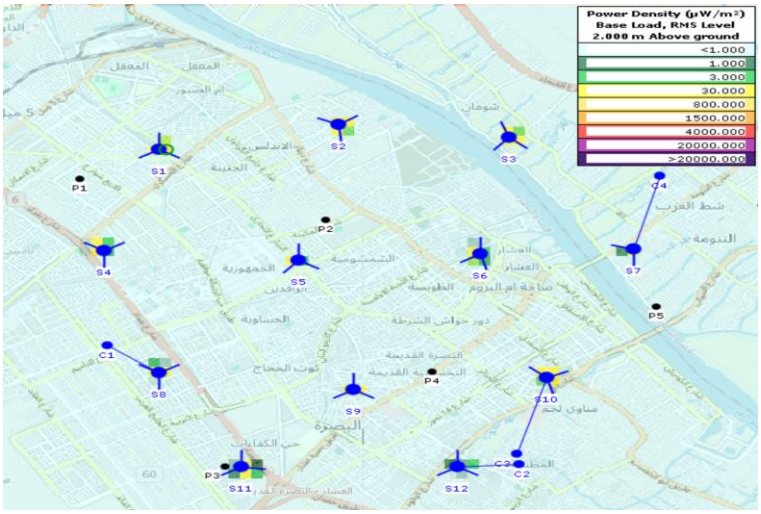

Figure 11. 3.6 GHz power density calculation at a base load

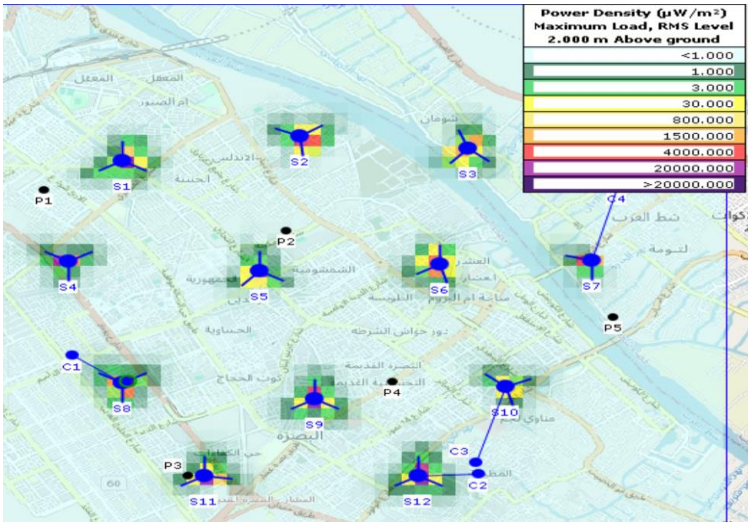

Figure 12. 3.6 GHz power density calculation at a max load

To start assessing network performance with this particular 5G band, 2m above ground coverage calculations are performed with 60° and 0° antennae down tilt as shown in Figure 13 and Figure 14, respectively. It is noticeable that sites with a 60° down tilt form a star-like shape to offer far but narrow coverage compared with a circle-like shape that presents wider coverage with fewer limited-service spots. Nevertheless, both degrees of antenna tilt perform reasonably well to offer excellent coverage across the majority of the network. Furthermore, it is evident that the coverage attained with the 2.1 GHz band is effectively better than that with 3.6 GHz shown in Figure 4. In consequence, the users across the 2.1 GHz network in general experience higher QoS than those with 3.6 GHz.

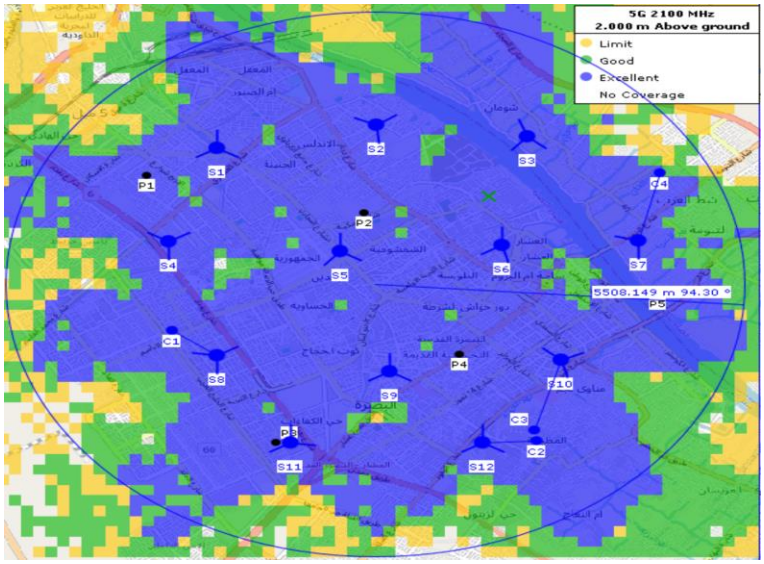

Figure 13. 2.1GHz coverage calculation at 60° down tilt

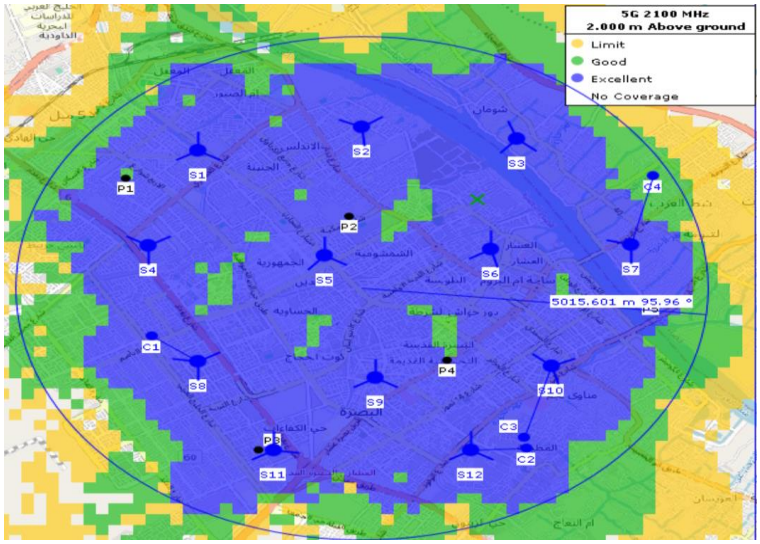

Figure 14. 2.1 GHz coverage calculation at 0° down tilt

The power measurements come next to evaluate the second design's behavior as shown in Figure 15 at 2 m above ground. Generally, the users are served with stronger signals as they get closer to the sites to achieve >-40 dBm. Compared with the 3.6 GHz design shown in Figure 8, the power levels attained with 2.1 GHz are higher with wider yellowish and greenish halos. A stronger signal allows for higher data rates, which translates to greater capacity. More users can be served simultaneously without experiencing significant degradation in service quality. To have more precise readings of power levels, Table 3 lists the power of five points (P1 through P5). The P3 and P4 represent the two extreme cases among others as the former point senses the highest power at -56.1 dBm whereas the latter records the lowest level at -107.9 dBm. That is dependent on the point's proximity to its serving site. In addition, there is an explicit improvement of points' power levels of the 2.1 GHz band compared with those of the 3.6 GHz shown in Table 1. For instance, P1 experiences the powers of -124.4 dBm and -102.8 dBm with 3.6 GHz and 2.1 GHz, respectively. Moreover, there is about 23 dBm of power level improvement for the P3 from moving down from the 3.6 GHz to the 2.1 GHz band.

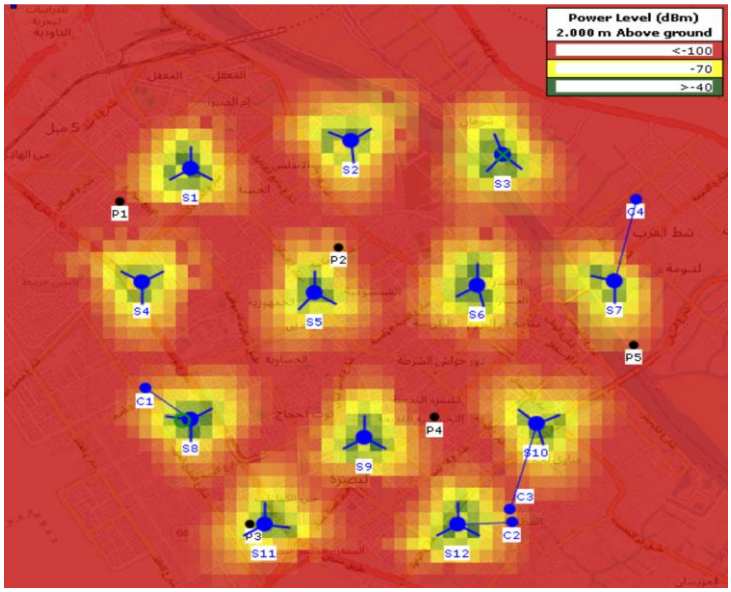

Figure 15. 2.1 GHz power calculation

Table 3: 2.1 GHz point power levels at 2m above ground

Point	Power (dBm)
P1	-102.8
P2	-103.1
P3	-56.1
P4	-107.9
P5	-100.3

After evaluating coverage and power, the interference levels are investigated for this frequency band network design as exposed in Figure 16. Each site's antenna shows blade-like regions shaded with green to reveal more than 20 dB of C/I which then degrades to yellow areas with 0 dB. Table 4 indicates the received power and C/I at several exact clients' placements. C2 experiences the best C/I at -6.8 dB with received power at -69.3 dB since it is served well by S12. On the other hand, C4 discloses a better C/I compared with C3 but with weaker received power because of its far location from S7. When comparing the clients' calculations in Table 2 and Table 4, it can be seen that all four clients witness enhancements in terms of both received power and interference levels when moved from 3.6 GHz to 2.1 GHz band.

Lastly, the RMS levels of the power density at 2 m above ground with the base traffic load are shown in Figure 17. As the figure reveals, power density across the vast majority of the network is kept at less than 1 $\mu W/m^2$. The areas near the sites record 1-3 $\mu W/m^2$ (i.e., greenish) that extend for a bit wider distance than those around sites in the 3.6 GHz in Figure 11. However, the power density levels are generally still reasonable across the 2.1 GHz network.

Table 4: 2.1 GHz clients' calculations

Client	Received Power (dB)	C/I (dB)
C1	-69.5	-7.7
C2	-69.3	-6.8
C3	-73.6	-13.9
C4	-84.3	-9.2

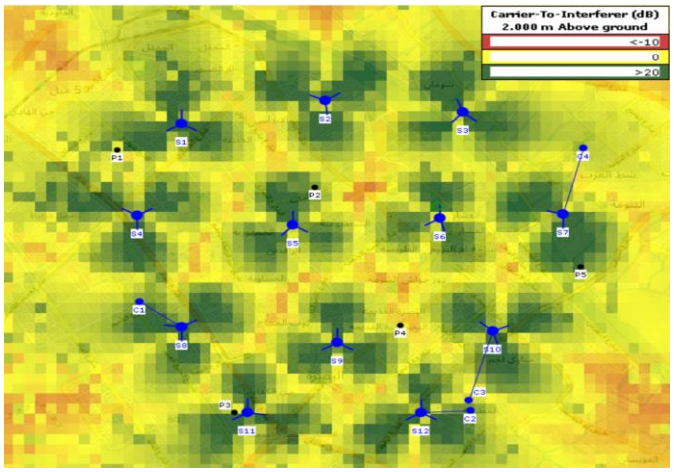

Figure 16. 2.1 GHz interference levels determination

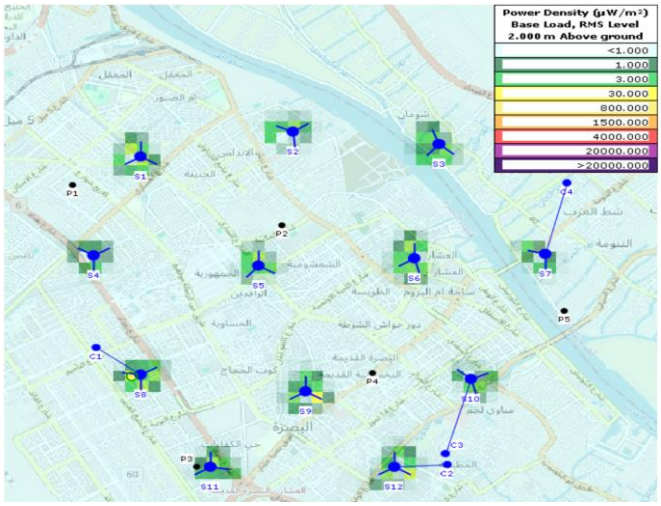

Figure 17. 2.1 GHz power density calculation

5.3 5G Network Deployment with 1.8 GHz Band

The deployed 5G frequency band is further reduced to 1.8 GHz in this section to study how the network performs compared with the other higher two bands presented previously. The antennae are mounted on sites at 35.2 m high and transmit signals with 43 dBm power which is less than the 3.6 GHz and 2.1 GHz designs by 10 dBm and 3 dBm, respectively. That decrease in transmission power is due to adopting a lower band in this design that in turn does not require as much power as the higher band networks.

The coverage theme of this design is measured 2 m above ground as revealed in Figure 18. Apparently, the coverage of the 1.8 GHz network proves its superiority compared with the preceding planned bands. That is because almost all of the targeted coverage circle of the 1.8 GHz network is shaded in blue with excellent coverage and better QoS which were not offered by the 3.6 GHz and 2.1 GHz designs. Furthermore, it is noticeable that the coverage overflows to exceed the target coverage area (i.e., the circle with a 5613m radius) that was set earlier for Basra city. Consequently, some sites and/or antennae can be removed to save network resources while maintaining coverage quality in the target area.

The power calculation theme at 1.8 GHz is shown in Figure 19. It is implicit that yellowish regions are extended to reflect stronger power levels. Moreover, wider power halos are offered by this band compared with the higher two bands presented in Figure 8 and Figure 15 to serve more users by the 1.8 GHz design. Furthermore, the points power calculation recorded in Table 5 exposes stronger levels between -63.9 dBm and -91.5 dBm for the five placed points across the network.

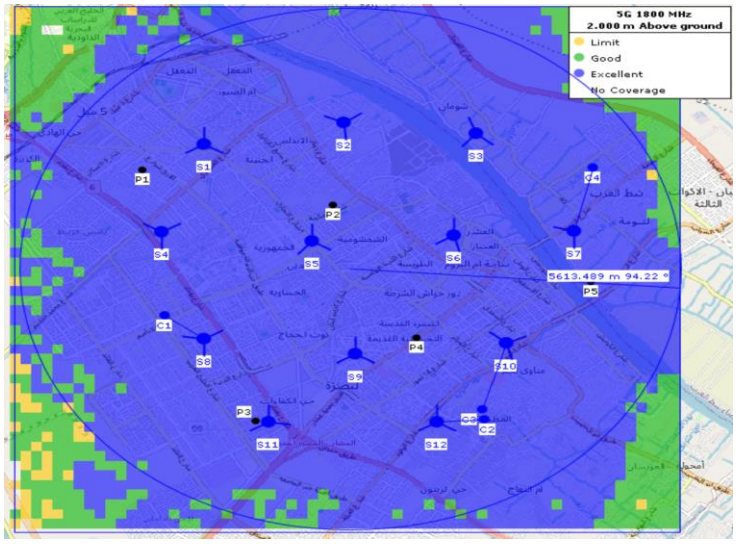

Figure 18. 1.8 GHz Coverage calculation

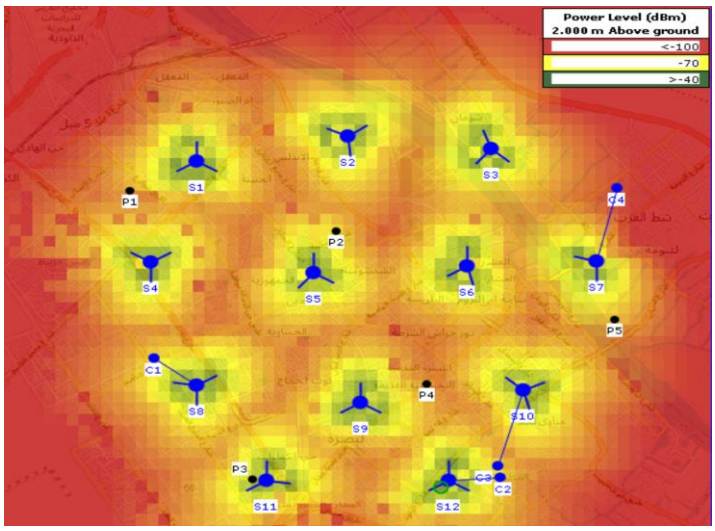

Figure 19. 2.1 GHz power calculation

By exploring the network interference as C/I, Figure 20 shows a wide view of the distribution over the 1.8 GHz design. The C/I levels are still greater than 20 dB close to sites and gradually turn to 0 dB in some far areas. In addition, users may experience some degradation due to interference when traveling among some orangish spots. To have a narrower view, Table 6 indicates that C1 senses the best C/I at -7.7 dB whereas C3 records the highest interference level at -13.9 dB. On the other hand, the RMS power density distribution is shown in Figure 21. It is apparent that except for the nearby areas around sites that reveal 1 $\mu W/m^2$, the power density level is kept at a minimum with even < 1 $\mu W/m^2$. Besides, when comparing this design's band with the previously deployed two bands, the 1.8 GHz network's power density levels in general show neutrality since it comes with wider halos than the 3.6 GHz but less density values than the 2.1 GHz networks. Overall, the power density is kept sufficiently low to avoid any harm to humans. That is because each of the IEEE [30], the International Commission on Non-Ionizing Radiation Protection (ICNIRP) [31], and the Federal Communications Commission (FCC) [32] have all specified a limit value for power density exposure to be 10 W/m^2 with frequencies 2 to 300 GHz for 30 minutes as an average time.

Table 5: 1.8 GHz point power levels at 2m above ground

Point	Power (dBm)
P1	-88.3
P2	-91.5
P3	-63.9
P4	-91.5
P5	-86.8

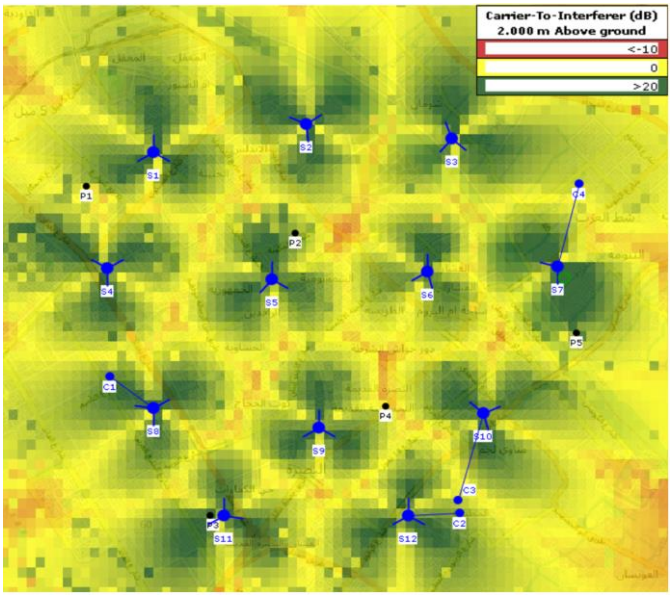

Figure 20. 1.8 GHz interference levels determination

Table 6: 1.8 GHz clients' calculations

Client	Received Power (dB)	C/I (dB)
C1	-60.5	-7.7
C2	-60.1	-8.8
C3	-63.4	-13.9
C4	-74.5	-12.1

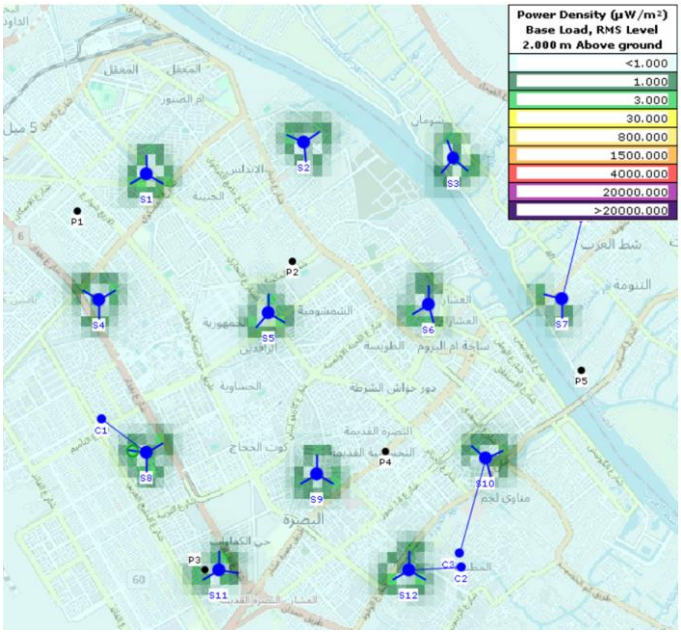

Figure 21. 1.8 GHz power density calculation

6. Conclusions

Radio network planning is effectively a crucial phase that precedes the implementation stage. This paper offered insights into 5G network deployment to identify the optimal frequency bands for 5G coverage and performance. Three of the FR1 5G bands (i.e., 1.8, 2.1, and 3.6 GHz) were applied in the proposed design based on a target area of Basra City. The study's outcomes recommend that the 3.6 GHz is chosen when the traffic load is at maximum, which is a rare case except for some public festivals and events where the population is high. That is because the power density in this band is kept at low safe levels. However, with a constrained level of power density, the 1.8 GHz proved its superiority among the rest of the bands since this 5G band offers better coverage, stronger signals, and lower interference levels. On the other hand, some limitations were addressed in this paper. First, the target area of Basra City could not be expanded since that required more sites to deploy but the used community edition of WiMAP is constrained to only 12 sites. Second, the simulation tool is restricted to only these three 5G bands which limits further exploration of higher FR2 (i.e., 24.25-52.6 GHz) deployment. As possible future works, rather than considering Basra City, the 5G networks can be generalized for other terrain-like regions. Additionally, the proposed designs may be further improved using different network optimization techniques such as beamforming, MIMO, power management algorithms, or machine learning approaches. In essence, the study helps network regulators and/or operators to determine the most appropriate spectral allocations for a smooth migration from 4G to 5G in Iraq.

References

[1] E. Dahlman, S. Parkvall and J. Skold, "4G: LTE/LTE-advanced for mobile broadband", *Academic press*, 2013.

[2] E. Hossain, M. Rasti, H. Tabassum, and A. Abdelnasser, "Evolution toward 5G multi-tier cellular wireless networks: An interference management perspective" *IEEE Wireless Communications*, vol. 21, no. 3, pp.118-127, 2014.

[3] R. Pawlak, P. Krawiec, and J. Zurek, "On measuring electromagnetic fields in 5g technology" *IEEE Access*, vol. 7, pp. 29826–29835, 2019, doi: 10.1109/ACCESS.2019.2902481.

[4] A. A. Zaidi, R. Baldemair, M. Andersson, S. Faxér, V. Molés-Cases, and Z. Wang, "Designing for the future: the 5g nr physical layer," *Ericsson Technology Review*, pp. 1-13, 2017.

[5] E. Dahlman, S. Parkvall, and J. Skold, "5G NR: The next generation wireless access technology," *Academic Press*, 2020.

[6] S. Faye et al., "A survey on emf-aware mobile network planning," *IEEE Access*, vol. 11, pp. 85927-85950, 2023, doi: 10.1109/ACCESS.2023.3297098.

[7] H.M. Tun, "Radio network planning and optimization for 5G telecommunication system based on physical constraints," *Journal of Computer Science Research*, vol. 3, no. 1, pp.1-5, 2021.

[8] S. Ahmadi, "5G nr–architecture, technology, implementation, and operation of 3gpp new radio standards", 1st ed. New York, NY, USA: Academic, 2019.

[9] Z. Khan, S. M. Khan, M. Chowdhury, M. Rahman and M. Islam, "Performance evaluation of 5g millimeter-wave-based vehicular communication for connected vehicles," *IEEE Access*, vol. 10, pp. 31031-31042, 2022, doi: 10.1109/ACCESS.2022.3158669.

[10] C. Sudhamani, M. Roslee, J.J. Tiang, A.U. Rehman, "A survey on 5g coverage improvement techniques: issues and future challenges," *Sensors*, vol. 23, no. 4, pp. 2356, 2023, doi: 10.3390/s23042356.

[11] B.K. Engiz and Ç. Kurnaz, "Comparison of signal strengths of 2g/3g/4g services on a university cpuams," *International Journal of Applied Mathematics Electronics and Computers*, no. 1, pp.37-42, September 2016.

[12] S.N. Shahab, T.S. Kiong and A.A. Abdulkaf, "A Framework for energy efficiency evaluation of lte network in urban, suburban and rural areas," *Australian Journal of Basic and Applied Sciences*, vol. 7, no. 7, pp.404-413, 2013.

[13] E.T. Tchao, J.D. Gadze and J.O. Agyapong, "Performance evaluation of a deployed 4g lte network," International Journal of Advanced Computer Science, vol. 9, no. 3, pp.165-178, 2018.

[14] A.M. Al-Kadhimi, "Performance evaluation of LTE and UMTS cellular networks in Iraq with multiple terrains" *Journal of Physics: Conference*

Series, vol. 1530, no. 1, pp. 012019, 2020, doi:10.1088/1742-6596/1530/1/012019.

[15] M. Alexandru, R. Urechiatu, "LTE indoor radio coverage optimization study in modern city environments," *Review of the Air Force Academy*, no. 2, pp.77, 2014.

[16] M.R.Fauzi, Sukiswo, and T. Prakoso, "Perencanaan Jaringan LTE Fdd 1800 Mhz Di Kota Semarang Menggunakan Atoll," *Transient: Jurnal Ilmiah Teknik Elektro*, vol. 4, no. 3, pp. 517-524, September 2015.

[17] J.A. Aldhaibani, A.Yahya, R.B.Ahmab, A.S. Md Zain, M.K.Salman and R.Edan, "On coverage analysis for lte-a cellular network," *International Journal of Engineering and Technology (IJET)*, vol. 5, no. 1, pp.492-497, 2013.

[18] R.Nlend and E.Tonye, "Planning and simulation of LTE radio network: case of the city of Yaoundé," *IOSR Journal of Electronics and Communication Engineering*, vol. 14, no. 2, pp.19-29, 2019, doi: 10.9790/2834-1402011929.

[19] S. Wang and C. Ran, "Rethinking cellular network planning and optimization," *IEEE Wireless Communications*, vol. 23, no. 2, pp. 118-125, Apr. 2016, doi: 10.1109/MWC.2016.7462493.

[20] S. K. Jha, R. Rokaya, A. Bhagat, A. R. Khan, and L. Aryal, "LTE network: coverage and capacity planning-4g cellular network planning around banepa," in *2017 International Conference on Networking and Network Applications (NaNA)*, Kathmandu, Nepal: IEEE, Oct. 2017, pp. 180-185. doi: 10.1109/NaNA.2017.23.

[21] M. Abdulhamid and K. Sayianka, "Performance of automatic frequency planning and optimization algorithm for cellular networks," *International Journal of Advanced Network, Monitoring and Controls*, vol. 8, no. 2, pp. 54-60, Jun. 2023, doi: 10.2478/ijanmc-2023-0056.

[22] M.M. Ahamed, S. Faruque, "5G network coverage planning and analysis of the deployment challenges" *Sensors*, vol. 21, no. 19, pp. 6608, 2021, doi: 10.3390/s21196608

[23] A. M. El-Hajj and T. Naous, "Radiation analysis in a gradual 5g network deployment strategy," *2020 IEEE 3rd 5G World Forum (5GWF)*, Bangalore, India, 2020, pp. 448-453, doi: 10.1109/5GWF49715.2020.9221314.

[24] G. Fahira, A. Hikmaturokhman and A. Rizal Danisya, "5G NR planning at mmwave frequency: study case in indonesia industrial area," *2020 2nd International Conference on Industrial Electrical and Electronics (ICIEE)*, Lombok, Indonesia, 2020, pp. 205-210, doi: 10.1109/ICIEE49813.2020.9277451.

[25] S. Kusmariyanto, D. Fadilla, F. H. Partiansyah, G. Asmungi and W. A. Priyono, "5G NR network planning in malang city east java using atoll software," *2022 11th Electrical Power, Electronics, Communications, Controls and Informatics Seminar (EECCIS)*, Malang, Indonesia, 2022, pp. 191-196, doi: 10.1109/EECCIS54468.2022.9902947.

[26] H. Beshley, M. Gregus, O. Urikova, I. Scherm, and M. Beshley, "Smart planning, design, and optimization of mobile networks ecosystem using ai-enhanced atoll software" *IEEE lnternational Conference on Advanced Trends in Radioelectronics, Telecommunications and Computer Engineering*, 2024, pp. 668-697, Cham: Springer Nature Switzerland. doi: 10.1007/978-3-031-61221-3_32

[27] R.S. Hassan, T. A. Rahman and A. Y. Abdulrahman, "LTE coverage network planning and comparison with different propagation models," *TELKOMNIKA*, vol.12, no.1, pp. 153-162, 2014.

[28] V. Erceg et al., "An empirically based path loss model for wireless channels in suburban environments," *IEEE Journal on Selected Areas in Communications*, vol. 17, no. 7, pp. 1205-1211, 1999, doi: 10.1109/49.778178.

[29] F.E. Shaibu et al., "Performance of path loss models over mid-band and high-band channels for 5G communication networks: A review," *Future Internet*, vol 15, no. 11, pp. 362, 2023, doi: 10.3390/fi15110362.

[30] IEEE C95. 1-2019, "IEEE standard for safety levels with respect to human exposure to electric, magnetic, and electromagnetic fields, 0 hz to 300 ghz," *Std C95.1-2019 (Revision of IEEE Std C95.1-2005/ Incorporates IEEE Std C95.1-2019/Cor 1-2019)*, pp. 1–312, 2019.

[31] International Commission on Non-Ionizing Radiation Protection, "Guidelines for limiting exposure to electromagnetic fields (100 khz to 300 ghz)," *Health Physics*, vol. 118, no. 5, pp. 483–524, 2020.

[32] Federal Communication Commission, "Report and order: Guidelines for evaluating the environmental effects of radiofrequency radiation," *FCC 96-326*, 1996.